University of Groningen

Levy walks evolve through interaction between movement and environmental complexity

de Jager, Monique; Weissing, Franz J.; Herman, Peter M. J.; Nolet, Bart A.; van de Koppel, Johan

IMPORTANT NOTE: You are advised to consult the publisher's version (publisher's PDF) if you wish to cite from it. Please check the document version below.

Document Version
Publisher's PDF, also known as Version of record

[Link to publication in University of Groningen/UMCG research database](#)

Supporting Online Material for

Lévy Walks Evolve Through Interaction Between Movement and Environmental Complexity

Monique de Jager,* Franz J. Weissing, Peter M. J. Herman, Bart A. Nolet, Johan van de Koppel

*To whom correspondence should be addressed. E-mail: m.dejager@nioo.knaw.nl

This PDF file includes:

Materials and Methods
Figs. S2.1 to S2.3
Tables S3.1 and S3.2
References and Notes
Caption for Movie S1

Other Supporting Online Material for this manuscript includes the following:
(available at www.sciencemag.org/cgi/content/full/332/6037/1551/DC1)

Movie S1
Matlab code for individual-based model of mussel movement (The MathWorks, Inc.)

Supporting Online Material for

Lévy walks evolve through interaction between movement and environmental complexity

Monique de Jager*, Franz J. Weissing, Peter M.J. Herman, Bart A. Nolet, Johan van de Koppel

*To whom correspondence should be addressed. Email: M.deJager@nioo.knaw.nl;

This PDF file includes

Materials and Methods

Figures S2.1 to S2.3

Tables S3.1 and S3.2

References

Other Supporting Online Material for this manuscript includes the following:
(available at www.sciencemag.org/cgi/content/full/...)

Movie S1

Matlab code (written for Matlab version 7.9.0 (R2009b © The MathWorks, Inc.))

Supporting Online Material

S1 Materials and Methods

S1.1 Characteristics of mussel movement

Although mussel movement becomes limited with increasing shell size, young mussels are good crawlers for many months after their metamorphosis (*S1*). During this period, mussels are able to search for conspecifics and aggregate. Once arrived at a good quality location, with respect to the number of neighbors and food availability, a mussel stops moving and attaches itself to the bed. When conditions become less suitable, a young mussel can still detach itself and search for a better location. This movement and attachment behavior at individual level directly affects the habitat quality for others, thereby leading to spatial patterning in mussel beds.

S1.2 Extraction of mussel movement data

Step lengths of young blue mussels (*Mytilus edulis*, 1.5-3 cm long) were obtained from experimental data of Van de Koppel *et al.* (2008, *S2*). The blue mussels used in these experiments were obtained from wooden wave-breaker poles near Vlissingen, the Netherlands. Experiments were performed in a 120x80x8 cm containers filled with unfiltered seawater. Mussels were placed on a 60x80 cm red PVC sheet. To record mussel movement, a Logitech QuickCam 9000 Pro webcam, which was positioned about 60 cm above the water surface and attached to a computer, photographed the mussels at 1 minute intervals for several hours. In total, 62 mussels were used for the experiments, resulting in 19,401 steps. Tracks of twelve of these mussels (12,401 steps) were obtained from isolation experiments, preventing the mussels from finding conspecifics and creating clusters. To investigate density-dependence, the tracks of the other 50 mussels (7,000 steps) were obtained from pattern formation experiments (see Fig. 1b). In pattern formation experiments, mussels are initially evenly distributed over the red PVC sheet, after which the mussels start to move and create patterns.

The first method that we used for the extraction of step lengths was to simply calculate the distance between two subsequent points using a 60 seconds interval. This time interval was chosen since our observations revealed that time intervals between 40 and 80 seconds are most adequate for monitoring mussel movements in our experiments.

In addition, we extracted step length distributions by applying two step length extraction methods suggested by Turchin (1998, *S3*). In the 'error radius method' (illustrated in Fig. S2.1a), the movements performed in n time intervals are aggregated into a single 'step' if the n-1 intermediate spatial positions are no more than a predefined distance x away from the line connecting the beginning of the movement to the end of it. When applying this method, the value of x was chosen by starting with a small value and then incrementing it iteratively until

35   oversampling was minimized, i.e., until autocorrelation in the turning angle vanished.
36   Autocorrelation was calculated with the acf function in R (R version 2.10.0 © 2009 The R
37   Foundation for Statistical Computing). When the autocorrelation of n data points exceeded the
38   confidence interval derived with the acf function, the distance x was increased by 0.01 cm.

39   Turchin's 'angle method' (illustrated in Fig. S2.1b) concerns the angle between movements. The
40   movements performed in n time intervals are aggregated into a single step if the angle between
41   the starting position and the end position is smaller than a predefined value $\beta_{max.}$. When this value
42   is exceeded after the nth movement, the corresponding point becomes the starting point for the
43   next step. The threshold value β_{max} was also chosen iteratively, starting with a small angle and
44   gradually increasing it until the autocorrelation in turning angles vanished.

45   As shown in Table S3.1, the method used for estimating step lengths does not affect our
46   conclusions: in all cases, the data are best explained by a Lévy walk, where the pure Lévy walk
47   model performs almost as well as a truncated Lévy walk. In all cases, R^2–values of the best-fitting
48   models exceed 0.995.

49   **S1.3 Fitting movement types to step length data**

50   The step length data of the mussel movements were used to create a step length frequency
51   distribution (Fig. 1a). When plotted on a log-log scale, a power-law probability distribution
52    $P(l) = Cl^{-\mu}$ results in a straight line with slope $-\mu$. However, drawing conclusions from this kind
53   of presentation can be deceptive (*S4-S6*). We therefore used a more robust method (*S5*) and first
54   determined the inverse cumulative frequency distribution of our data, which for each step length l
55   gives the fraction of steps with lengths larger or equal to l. This cumulative distribution is plotted
56   in Fig. 1b on a log-log scale. We compared this distribution with the cumulative probability
57   distribution of three random movement strategies: Brownian walk, Lévy walk, and truncated Lévy
58   walk.

59   ***Brownian walk***

60   Brownian walk is a random movement strategy that corresponds to normal diffusion. The step
61   length distribution can be derived from an exponential distribution with $\lambda > 0$:

62    $$f(l) = \lambda e^{-\lambda l}. \tag{1}$$

63   ***Lévy walk***

64   The frequency distribution of step lengths that characterizes a Lévy walk has a heavy tail and is
65   scale-free, i.e. the characteristic exponent of the distribution is independent of scale. To fit a Lévy
66   walk to the data, a Pareto distribution (*S7*) was used:

67    $$f(l) = C_{\mu} l^{-\mu}. \tag{2}$$

68   The shape parameter μ (which has to exceed 1) is known as the Lévy exponent or scaling exponent
69   and determines the movement strategy (see Fig. S2.2). When μ is close to 1, the resulting
70   movement strategy resembles ballistic, straight-line motion, as the probability to move a very
71   large distance is equal to the chance of making a small displacement. A movement strategy is
72   called a Lévy walk when the scaling exponent is between 1 and 3. When μ approaches 1, the
73   movement is approximately ballistic, while it is approximately Brownian when μ approaches 3
74   (and for $\mu > 3$). The Lévy walks found in nature typically have an exponent μ of approximately 2
75   (S4, S8-S10). C_μ is a normalization constant ensuring that the distribution $f(l)$ has a total mass
76   equal to 1, i.e. that all values of $f(l)$ sum up to 1. If we impose the additional criterion that steps
77   must have a minimum length $l_{min}(0 < l_{min} < l)$, this constant is given by

78    $$C_\mu = (\mu - 1)l_{min}^{\mu-1} .$$ (3)

79   When fitting our data to a Lévy walk, we used the value of l_{min} that provided the best fit of the
80   step length distributions to the actual data.

81   ***Truncated Lévy walk***

82   A truncated Lévy walk differs from a standard Lévy walk in the tail section of the frequency
83   distribution; a truncated Lévy walk has a maximum step size and, as a consequence, loses its
84   infinite variance and scale-free character at large step sizes. The truncated Lévy walk was
85   represented by the truncated Pareto distribution, which can be described by the same function
86    $f(l)$ as a standard Pareto distribution, but with different constant C_μ:

87    $$C_\mu = \frac{\mu - 1}{l_{min}^{1-\mu} - l_{max}^{1-\mu}} .$$ (4)

88   In a truncated Lévy walk, step lengths are constrained to the interval $l_{min} < l < l_{max}$. When
89   fitting our data to a truncated Lévy walk, we used those values of l_{min} and l_{max} that yielded the
90   best fit of the movement models to the data (l_{min} = 0.42 cm and l_{max} = 58.84 cm).

91   ***Goodness-of-fit and model selection***

92   For the frequency distributions mentioned above, the fit to the step length data of solitary mussels
93   was calculated using Maximum Likelihood estimation by fitting the inverse cumulative frequency
94   distribution to that of the experimental data. By comparing the inverse cumulative distributions to
95   that of the data, Goodness-of-fit (G) and the Akaike Information Criterion (AIC) were calculated as
96   well as the variance explained by the fitted model (R^2). The Goodness-of-fit method measures how
97   well the experimental data follows the frequency distributions of the movement strategies; the fit
98   is best when the G-value is closest to zero. The Goodness-of-fit value is calculated as

99    $$G = 2 \sum O_i \ln \left(\frac{O_i}{E_i}\right),$$ (5)

100 where O is the inverse cumulative distribution of the experimental data and E is that of the fitted
101 movement strategies. We used the inverse cumulative distribution as this is the most robust
102 method to compare the observed and expected distributions (*S5*). The highest AIC weight, which is
103 calculated by comparing the AIC values, and the highest R^2 correspond to the movement type best
104 fitting the actual data (*S11*). This method was used for the analysis of the movement strategies of
105 the 12 solitary mussels, both individually and as a whole, using the step lengths obtained per
106 minute as well as those derived with the two methods of Turchin (see Fig. S2.1). Additionally, step
107 lengths obtained from pattern formation experiments were grouped for different combinations of
108 local density (within a radius of 3.3 cm) and long-range density (within a radius of 22.5 cm). These
109 groups of step lengths were used for determining the Lévy exponent at different densities, in
110 order to observe whether a composite Brownian walk exists in mussel movement (see Table S3.2).

111 **S1.4 Computer Simulations**

112 *Individual based model*

113 We developed an individual based model that describes pattern formation in mussels by relating
114 the chance of movement to the short- and long-range densities of mussels, following Van de
115 Koppel *et al.* (2008, *S2*). Whereas they modeled pattern formation in mussel beds by adjusting the
116 movement speed to the short- and long-range densities (*S2*), we extracted the stop and move
117 behavior of the mussels from the experimental data. In our model, 2500 'mussels' (with a radius of
118 1.5 cm each) are initially spread homogeneously within a 150 cm by 150 cm arena. Each time step,
119 the short-range (D_1) and long-range (D_2) densities are determined for each individual, based on
120 mussel densities within a radius of 3.3 cm and 22.5 cm, respectively. These radii correspond to the
121 ranges in which we found significant correlations with the probability of moving in a multi-variate
122 regression analysis of our experimental data (F = 77.17, p << 0.001, R^2 = 0.622, df = 136). The
123 probability P_{move} that a mussel moves is negatively related to the short-range density D_1 and
124 positively related to the long-range density D_2 (see Fig. S2.3), which causes mussels to stay in
125 places where they can aggregate with direct neighbors, but move away from crowded locations
126 where food becomes limiting. In the model, we used a linear relationship between P_{move} and the
127 two densities:

128 $$P_{move} = a - bD_1 + cD_2, \tag{6}$$

129 which was obtained by applying linear regression to our experimental data (*a* = 0.63, *b* = 1.26, and
130 *c* = 1.05). If a mussel decided to move in our model, its step length *l* was chosen at random from a
131 power law distribution (*S12*) with a given Lévy exponent μ > 1:

132 $$l = l_{min}(1 - x)^{-\frac{1}{\mu - 1}}, \tag{7}$$

133 where *x* is a random variable that is uniformly distributed over the unit interval (0 ≤ x ≤ 1), and
134 l_{min} is the minimum distance traveled when moving (*S7*), which we have set at 0.3 cm. Each

135 simulation step, mussels move instantaneously from one location to another, though step lengths
136 were truncated when a movement path was obstructed by another mussel. This truncation was
137 calculated by determining the free movement path until collision, using a band width of 3 cm (the
138 size of a mussel) around the line segment connecting the mussels' original location to its intended
139 destination. When a conspecific was located within this band, the mussel stopped in front of this
140 conspecific, thereby truncating its movement path. All movements occurred simultaneously and
141 all individuals in a simulation used the same movement strategy.

142 As differences occur in the average distance covered per simulation step between the movement
143 strategies (ballistic individuals move a larger distance per simulation step than Lévy or Brownian
144 walkers) and assuming that movement speed is constant, more time is needed for a ballistic step
145 than for a Brownian step. To avoid having Brownian movers switch more frequently between
146 moving and stopping than ballistic movers, we updated the state of either moving or stopping not
147 after each simulation step but after an average distance moved.

148 A simulation was finished when the average short-range density exceeded 1.5 times the mean
149 long-range density. At that moment, the total distance travelled was recorded. As we assume that
150 the movement speed is constant, the rate of patterning is proportional to the normalized inverse
151 of the distance traversed until a pattern is formed. Simulations were run for a range of Lévy
152 exponents ($1 < \mu \leq 3$), and for each value the rate of pattern formation was plotted as a function of
153 μ. The model was implemented in Matlab version 7.9 (©1984-2009. The MathWorks, Inc.).

154 ***Evolutionary model***

155 Evolutionary change was studied in a monomorphic resident population by investigating whether
156 the fitness of rare mutants is higher than that of the residents, implying that the mutants can
157 increase in frequency (*S13*, S14). After the mussels moved an equal distance, we recorded the
158 short-range density, the long-range density, and the fraction of mussels that was still moving, for
159 both the residents and the mutants. In a population with non-overlapping generations, fitness is
160 given by the product of survival probability and fecundity. We assumed that survival probability is
161 proportional to the local mussel density D_1 and that fecundity is inversely proportional to the long-
162 range density D_2 (as this density affects food supply) and to the time *X* spent on moving (as energy
163 spent on moving cannot be invested in offspring production). Dividing the fitness measures thus
164 obtained for a mutant and a resident results in a measure for the relative fitness of the mutant
165 strategy:

166 $$F_{mut} = \frac{D_{1,mut}}{D_{1,res}} * \frac{D_{2,res}}{D_{2,mut}} * \frac{X_{res}}{X_{mut}} .$$ (8)

167 Mutant strategies with a relative fitness value larger than one will invade and potentially take over
168 the resident population. For any combination of resident and mutant movement strategy, the
169 relative fitness of the mutants is depicted in a pairwise invasibility plot (*S14*, see Fig. 3). In this plot,

170   the color red indicates that the mutant has a higher fitness than the resident ($F_{mut} > 1$), while the
171   color green indicates that the mutant cannot invade the resident population ($F_{mut} < 1$). The
172   intersection of the line separating these two scenarios ($F_{mut} = 1$) with the main diagonal of the
173   pairwise invasibility plot corresponds to an evolutionarily singular strategy (*S13, S14*).
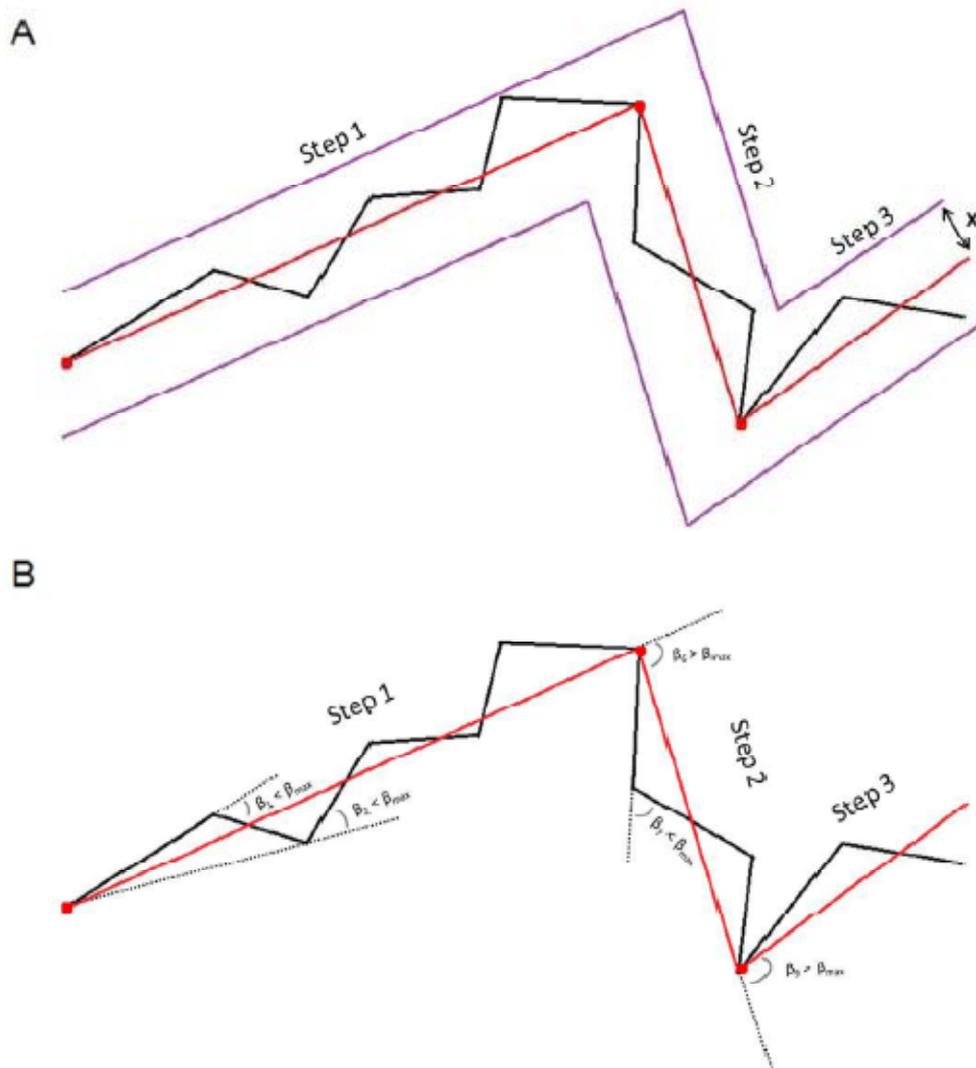
S2 Supporting Online Figures

Fig. S2.1. Step length calculation using the 'error radius method' (A) and the 'angle method' (B). In the first method **(A)**, *n* steps are aggregated into one move if the *n*-1 intermediate spatial positions are no more than *x* units away from the line connecting the beginning of the step to the end of it. The second method **(B)** is based on reorientation events; when the angle β (between the dotted black line and the solid black line) exceeds a certain threshold value, the corresponding point is the next new point (after Turchin, 1998; *S3*).
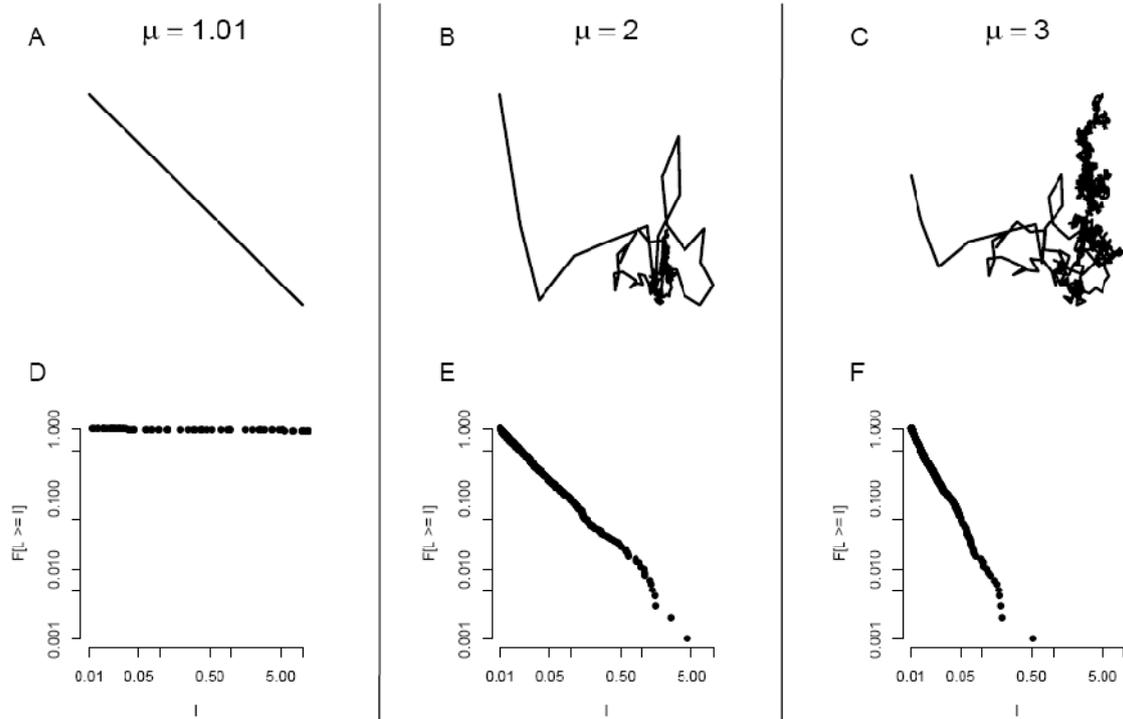
Fig. S2.2. The Lévy exponent μ determines the shape of the step length distribution and thus the movement strategy. When μ is close to 1, the movement strategy resembles ballistic, straight-line motion (**A, D**), whereas the step length distribution is similar to that of a Brownian walk when μ approaches 3 (**C, F**). The movement strategy is referred to as a Lévy walk when $1 < μ < 3$ (**B, E**). **A**, **B**, and **C** show movement trajectories obtained with μ = 1.01, 2, and 3, respectively. The inverse cumulative step length frequency distributions (i.e. the fraction of steps that is larger than or equal to the displacement length (l) that is given on the x-axis) are given by **D**, **E**, and **F** for μ = 1.01, 2, and 3, respectively.
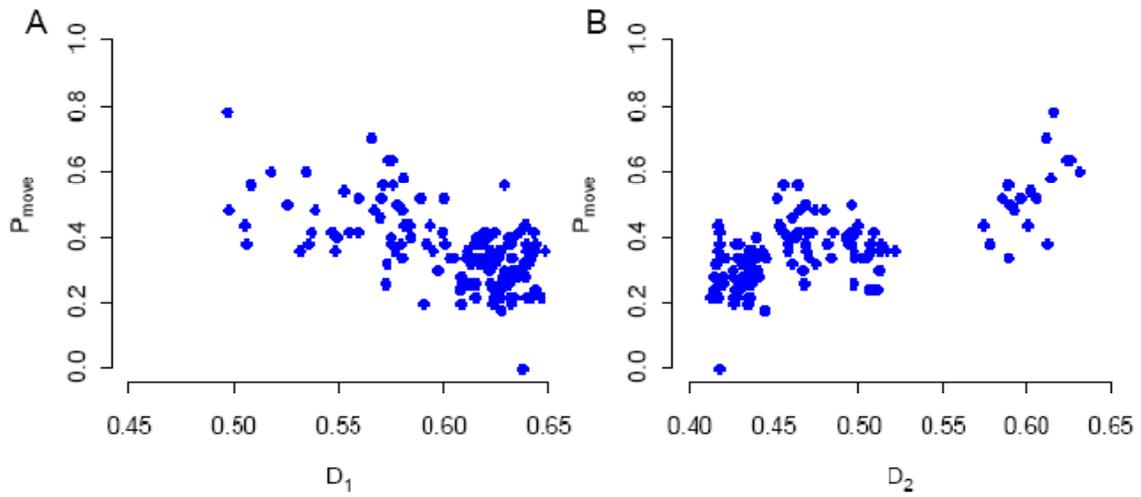
Fig. S2.3. Experimental data shows that the probability of moving depends on short-range and long-range mussel densities. (A) Local mussel density decreases the probability of moving; mussels tend to stay in denser clumps. **(B)** The probability of moving positively correlates with long-range density; mussels move away from areas where competition is high.

S3 Supporting Online Tables

Table S3.1. Summary of the model fits to the step length data. Goodness-of-fit (G), AIC weights and % variance explained of each movement strategy fitted to the mussel data (R^2) for all three methods that were used to obtain the step lengths. Truncated Lévy walk (TLW) corresponds best to the raw data and the data obtained using the error radius method. Data acquired with the angle method was best described by a Lévy walk (LW). Lévy exponents ranged from 1.930 to 2.174, with a mean µ of 2.032.

Method	Model	G	AIC weights	Adjusted R^2	Lévy exponent
Step per minute	Truncated Lévy walk	33.60	0.446	0.999	2.127
	Lévy walk	64.54	0.431	0.999	2.174
	Brownian walk	-119.43	0.123	0.878	-
Error radius method	Truncated Lévy walk	-2.69	0.437	0.997	1.967
	Lévy walk	3.93	0.401	0.995	2.045
	Brownian walk	-344.85	0.163	0.898	-
Angle method	Truncated Lévy walk	36.43	0.445	0.995	1.930
	Lévy walk	73.20	0.453	0.996	1.946
	Brownian walk	-106.00	0.103	0.734	-

Table S3.2. Lévy exponent during pattern formation. Lévy exponents for step lengths in different local and long-range density groups, for all three methods that were used to obtain the step lengths. Low/Low = both low local and long-range densities; Low/High = low local and high long-range density; High/Low = high local and low long-range density; High/High = both high local and long-range densities. Pattern formation in mussel beds produces an environment with high local densities and low long-range densities. There is no significant correlation between Lévy exponent and the degree of patterning, as well as any other relationship between the exponent and mussel density; we can therefore reject the hypothesis of a composite Brownian walk, where movement speeds are adjusted to local environmental conditions (*S15-S18*).

Method	Low/Low	Low/High	High/Low	High/High
Step per minute	2.05	2.05	2.06	2.05
Error radius method	2.00	2.07	2.05	2.05
Angle method	2.00	2.00	2.00	2.00

S4 Supporting Online References

S1.   R. A. Maas Geesteranus, *Arch Neerl Zool* **6**, 283 (1942).
S2.   J. van de Koppel *et al*., *Science* **322**, 739 (2008).
S3.   P. Turchin, *Quantitative Analysis of Movement*. (Sinauer Associates, 1998).
S4.   D. W. Sims, D. Righton, J. W. Pitchford, *J. Anim. Ecol.* **76**, 222 (2007).
S5.   A. M. Edwards *et al*., *Nature* **449**, 1044 (2007).
S6.   E. P. White, *Ecology* **89**, 2971 (2008).
S7.   A. Clauset, C. R. Shalizi, M. E. J. Newman, *SIAM Rev*. **51**, 661 (2009).
10.   G. Ramos-Fernandez et al., Behav. Ecol. Sociobiol. 55, 223 (2004).
11.   A. M. Reynolds et al., Ecology 88, 1955 (2007).
12.   N. E. Humphries et al., Nature 465, 1066 (2010).
S11.   K. P. Burnham, D. R. Anderson, *Model selection and multimodel inference: A practical information-theoretic approach* (Springer-Verlag, 2002).
S12.   M.E.J. Newman, *Contemp. Phys.* **46**, 323 (2005).
S13.   S. A. H. Geritz, E. Kisdi, G. Meszena, J. A. J. Metz, *Evol. Ecol.* **12**, 35 (1998).
S14.   F. Dercole, S. Rinaldi, *Analysis of evolutionary processes: the adaptive dynamics approach and its applications* (Princeton University Press, 2008)
S15.   S. Benhamou, *Ecology* **88**, 1962 (2007).
S16.   A. Reynolds, *Ecology* **89**, 2347 (2008).
S17.   S. Benhamou, *Ecology* **89**, 2351 (2008).
S18.   B. A. Nolet, W. M. Mooij, *J. Anim. Ecol.* **71**, 451 (2002).

Movie S1

1201187S1.mov: Time-laps movie showing the movement behavior of a single mussel, with the corresponding movement track plotted as the mussel is moving. The video covers nearly a two hour time period (QuickTime movie, 11 MB), with images taken every 10 seconds. We acknowledge Aniek van den Berg for running this movement experiment.

Matlab code:

IBM1201187S1.m: Individual Based model of mussels moving into a self-organized pattern. The code was written for Matlab version 7.9.0 (R2009b © The Mathworks, Inc.) and shows the distribution of mussels after each simulation step.